Neurobiology of Aging 77 (2019) 44–57

Contents lists available at ScienceDirect

Neurobiology of Aging

journal homepage: www.elsevier.com/locate/neuaging

Age-related differences in neural spectral power during motor learning

Laura Milena Rueda-Delgado [a,*], Kirstin Friederike Heise [a], Andreas Daffertshofer [b], Dante Mantini [a,c], Stephan Patrick Swinnen [a,d]

[a] KU Leuven, Department of Movement Sciences, Movement Control and Neuroplasticity Research Group, Leuven, Belgium
[b] Amsterdam Movement Sciences and Institute for Brain and Behaviour, Faculty of Behavioural and Movement Sciences, Department of Human Movement Sciences, Vrije Universiteit Amsterdam, Amsterdam, the Netherlands
[c] Functional Neuroimaging Laboratory, IRCCS San Camillo Hospital Foundation, Venice, Italy
[d] KU Leuven, Leuven Brain Institute (LBI), Leuven, Belgium

ARTICLE INFO

Article history:
Received 20 April 2018
Received in revised form 29 November 2018
Accepted 27 December 2018
Available online 6 January 2019

Keywords:
Motor learning
Aging
Spectral analysis
Electroencephalography
Linear mixed-effects model

ABSTRACT

We investigated how older adults preserve the capability to acquire new motor skills in the face of age-related brain alterations. We assessed neural changes associated with learning a bimanual coordination task over 4 days of practice in healthy young (n = 24) and older adults (n = 24). The electroencephalogram was recorded during task performance at the start and end of training. Motor performance improved with practice in both groups, but the amount of learning was lower in the older adults. Beta power (15–30 Hz) in sensorimotor and prefrontal cortices of older adults was reduced with training, indicative of higher neural activity. We also found a functional reorganization after training in beta and alpha (8–12 Hz) bands. Between-session changes in alpha and beta power differed between groups in several cortical areas: young adults exhibited reduced power in the beta band in sensorimotor cortices, whereas older adults displayed a smaller decrease. Our findings indicate a less flexible reorganization of neural activity accompanying learning in older adults compared with young adults.

1. Introduction

A key mechanism for maintaining functional independence with aging is the learning of new skills. The level at which older adults learn a motor skill depends on the type of task, the feedback (FB) provided, and the duration of practice, more than for the younger adults (Davis et al., 2015; Swinnen et al., 1997; Voelcker-Rehage, 2008). Learning is thought to rely on the ability of neuronal assemblies to modify their structure and function with specific stimuli or environmental exposure, that is, neuroplasticity (Pascual-Leone et al., 2011; Ramón y Cajal, 1904). Neural markers of this process have been identified with magneto/electroencephalography (M/EEG), that is, noninvasive measures of neural activity with high temporal resolution. In young adults, beta power (~12–30 Hz) over primary sensorimotor cortices (M1/S1) decreases after sequence learning (Andres et al., 1999; Cunha et al., 2006; Pollok et al., 2014) and learning a bimanual polyrhythmic isometric force task (Boonstra et al., 2007; Houweling et al., 2010b). Similarly, alpha power (~8–12 Hz) decreases over M1/S1 accompany sequence learning (Andres et al., 1999; Bönstrup et al., 2015; Zhuang et al., 1997) and unilateral visuomotor learning (Veldman et al., 2018).

Decreases of power in the alpha and beta bands over sensorimotor areas are arguably indexes of higher neural activity (Jantzen et al., 2001; Pfurtscheller and Lopes da Silva, 1999; Pfurtscheller, 2001) and reflect activity of interconnected pyramidal and inhibitory interneurons in sensorimotor regions (Hall et al., 2011; Muthukumaraswamy et al., 2013; Pfurtscheller and Lopes da Silva, 1999; Rossiter et al., 2015). Modulations of central alpha are thought to be generated by the interaction of thalamocortical relay neurons and reticular nucleus neurons (Lopes da Silva, 2006). Experimental work suggests that the beta rhythm is primarily visible in the sensorimotor cortex, although modeling work suggests its origin in corticothalamic loops (Aburn et al., 2012; Lopes da Silva, 2010; Moran et al., 2007; Salmelin and Hari, 1994). The relevance of the beta band during movements has been repeatedly emphasized across studies (Gross et al., 2005; Mima et al., 2000; Serrien and Brown, 2002; Serrien et al., 2003; van Wijk et al., 2012).

Present address: Trinity College Dublin, Trinity College Institute of Neuroscience, Lloyd Building, College Green, Dublin 2, Ireland.
* Corresponding author at: KU Leuven, Department of Movement Sciences, Movement Control and Neuroplasticity Research Group, Tervuurse Vest 101, Leuven 3001, Belgium. Tel.: 32 16 329071; fax: 32 16 329197.
E-mail address: ruedadlm@tcd.ie (L.M. Rueda-Delgado).

0197-4580/$ – see front matter © 2019 Elsevier Inc. All rights reserved.
https://doi.org/10.1016/j.neurobiolaging.2018.12.013

Most studies have focused on spectral changes after a single session of practice of motor sequences or unimanual movements with augmented feedback (FB). Single sessions may be affected by factors exogenous to the experimental design, such as fatigue, mood, or attention (Cahill et al., 2001). Accordingly, it remains unclear how spectral components change after a longer practice regime that fosters learning and diminishes the temporary impact of exogenous factors to the experimental design. In addition, FB-guided motor sequences or unimanual movements ensure that the learning occurs within a short period and requires limited involvement of nonmotor brain functions (Dayan and Cohen, 2011). In contrast, learning a complex bimanual skill requires the slow acquisition of a new map to control interlimb dynamics, with the involvement of both motor and cognitive functions (Debaere et al., 2004; Puttemans et al., 2005; Remy et al., 2008; Ronsse et al., 2011; Santos Monteiro et al., 2017). Thus, in this study, we used bimanual movements as a prototype of a complex skill to investigate the interplay of brain functions associated with learning across several days.

To note, M/EEG spectral measures are also dependent on age. Studies have revealed lower alpha and beta power in older compared with young adults in M1/S1 during unimanual movements (Gaetz et al., 2010; Mattay et al., 2002; Rossiter et al., 2014; Sailer et al., 2000; Schmiedt-Fehr et al., 2016). Moreover, reduced lateralization of the topographical pattern in alpha is found in older compared with young adults during unimanual tasks (Labyt et al., 2004, 2006; Vallesi et al., 2010). These studies indicate an “overactivation” in older adults to execute simple tasks.

Although M/EEG has provided evidence that functional reorganization occurs after minutes or hours of practice in young adults, the limits of this reorganization in the context of aging have hardly been explored. It has been shown that after 30-min practice of a unilateral motor sequence, age-related effects were found in the alpha band but not in the beta band in M1/S1 (Mary et al., 2015). Insight into age effects on learning can aid the design of therapies to improve the dexterity of older adults. For the first time, we investigated how training of a complex bimanual coordination task induces age-dependent neural changes in alpha and beta bands.

To this end, we used cutting-edge methods by recording high-density EEG signals and reconstructing the neural sources of alpha and beta activity using individual head models. In general, source reconstruction can be considered to yield a higher accuracy than sensor-level analyses (Hallez et al., 2007). We expected age-associated neuroanatomical alterations to impact functional brain activity and training-induced plasticity. We hypothesized lower alpha and beta power in sensorimotor areas in the older versus young group, presumably reflecting higher neural activity in the former group. With respect to training-induced plasticity, we expected a common mechanism to be visible in both groups, that is, learning-induced decreases of alpha and beta power in sensorimotor areas. Because previous reports with transcranial magnetic stimulation and functional magnetic resonance imaging (fMRI) revealed age-related differences in training-induced plasticity also in nonsensorimotor areas (Aizenstein et al., 2006; Berghuis et al., 2016; Erickson et al., 2007; Lin et al., 2012), we anticipated age-related differences in this broader cortical territory as well.

2. Materials and methods

2.1. Participants

Forty-eight participants were recruited: 24 young (11 male; mean age 26 years; range 21–32 years) and 24 older adults (14 male; mean age 67 years; range 60–74 years). All participants were right-handed according to the Oldfield Handedness Questionnaire (Oldfield, 1971), except for one older participant (young group: mean 91.4, range 53–100; older group: mean 92.6, range 24–100). Participants were not professional musicians and had no history of neurological disease and no injury to the wrists. Older participants scored on average 28.08 (SD = 1.98) in the Montreal Cognitive Assessment test (MOCA) (Nasreddine et al., 2005). MOCA scores of less than 26 are considered indicative of mild cognitive impairment (Davis et al., 2015). Four older participants who scored exactly 25 in the MOCA test were excluded from the analysis. Participants provided written informed consent to the study, which had been approved by the Ethics Committee of KU Leuven.

2.2. Setup and task

Participants practiced a bimanual visuomotor task similar to the one previously used in our laboratory (Beets et al., 2015; Gooijers et al., 2013; Pauwels et al., 2014; Rueda-Delgado et al., 2017; Sisti et al., 2011; Solesio-Jofre et al., 2014). They were seated in front of a computer with their forearms resting on 2 ramps covered with foam for comfort. A shaft embedded into a rotating disc was placed at the end of each ramp. The rotating disc was glued to a shaft encoder for registration of angular displacement (Avago Technologies, sampling frequency of 250 Hz and accuracy of 0.089°). Participants were instructed to hold the dials with their thumb and index fingers. A wooden frame was positioned on top of the participants' limbs to prevent them from seeing their hands/forearms. The data from the angular encoders were recorded and analyzed with LabView 8.5 (National Instruments, Austin, Texas, USA).

Task and FB are illustrated in Fig. 1A. The rotation of the dials, one for each hand, moved a red cursor on the screen. The task consisted of the cyclical rotation of the dials at different speeds for each hand during 8 seconds. Depending on the session, the cursor was visible only after the trial was finished (after-trial FB) or was not visible at all (no FB). Clockwise rotation of the right dial moved the cursor to the right upper corner; counter clockwise rotation moved the cursor to the left lower corner. Clockwise rotation of the left dial moved the cursor to the left upper corner; counter clockwise rotation moved the cursor to the right lower corner. Simultaneous rotation of both dials resulted in drawing lines with different slopes, depending on the direction of the rotation and the speed. A blue line was shown on the screen as a cue for the required pattern. A line on the vertical axis indicated a synchronous/symmetric movement of the hands (isofrequency movement or 1:1 ratio). A line with a positive slope on the right side of the vertical axis indicated a nonisofrequency rhythm of 2:5, where the right hand kept the fast pace. By contrast, a line with a negative slope on the left side of the vertical axis indicated the mirrored rhythm of 5:2, where the left hand kept the fast pace (see Fig. 1A). A white dot moved along the cue line for 8 seconds, indicating the tempo at which the movement should be undertaken. The goal of the task was to rotate the dials in such a way that the line drawn by the participant would match the cue line in both inclination (coordination) and length (tempo). In the isofrequency condition, the required frequency of speed was 1 Hz, whereas in the nonisofrequency conditions (2:5 and 5:2), was 0.8 Hz for the slow and 2 Hz for the fast hand. One rotation of the disc corresponded to a translation of the cursor of approximately 0.64 cm.

Participants had control over the start of the trial by moving the dials back to the north position and holding them there for 2 seconds. A trial started with the line shown on the screen and a yellow circle in the starting position indicating that no movement was required. Once the yellow circle disappeared, the white dot started moving along the line triggering movement initiation. The execution of the movement, set by the motion of the white dot, lasted 8 seconds (see Fig. 2). For the sessions in which after-trial FB was

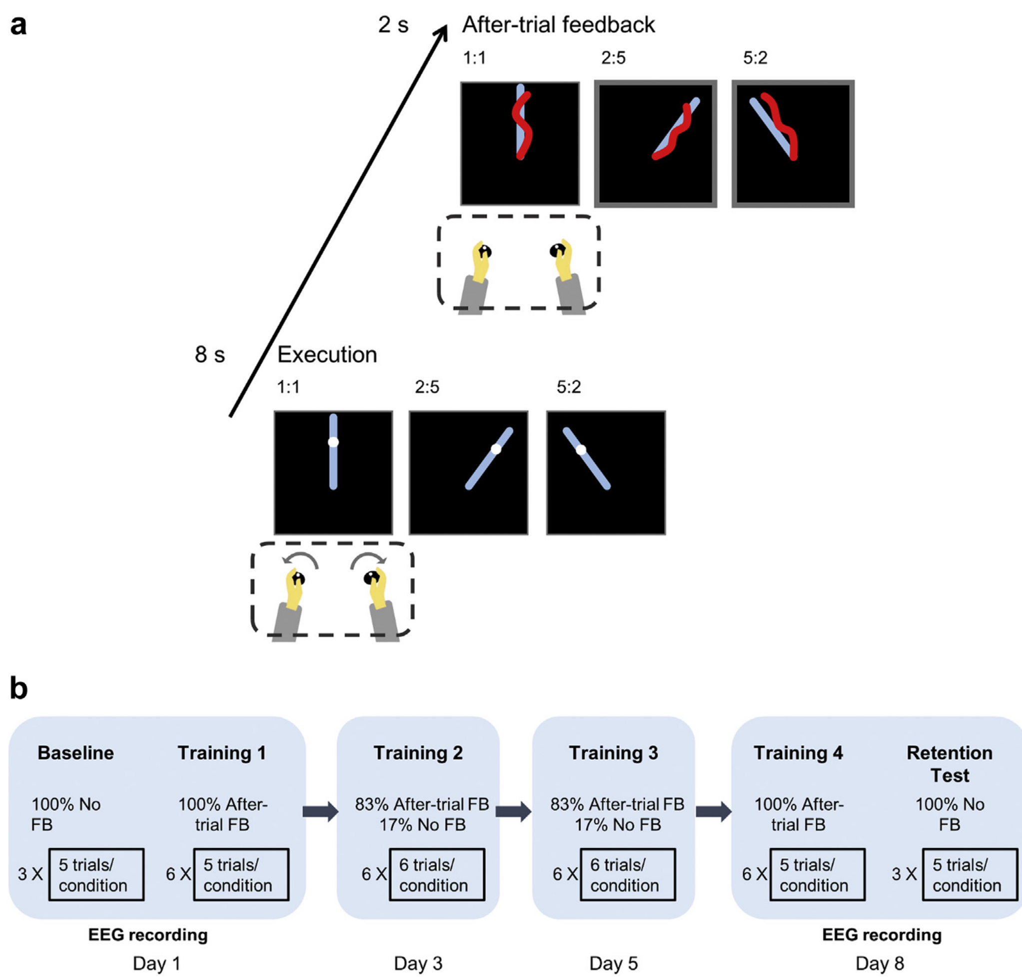

Fig. 1. (A) Participants executed outward rotations of their wrists with no visibility of their own movements or online feedback. After execution, participants received visual feedback. Dotted line indicates the wooden frame that blocked the visibility to the participants' hands. (B) Training program of 4 days, distributed over 8 calendar days with 2–3 days in between. Abbreviations: FB, feedback; EEG, electroencephalogram.

given, the resulting line drawn from the bimanual movement was shown along with the cue line for 2 seconds. This protocol allowed for provision of augmented FB (on the PC screen) in addition to the naturally available sensory information sources. However, this FB was not provided concurrently with actual performance of the movement to reduce dependence on this source of augmented visual information for online steering of the coordination pattern (Magill, 2007; Ronsse et al., 2011; Schmidt, 1991; Schmidt and Lee, 2011). In the no FB sessions, this information was not provided. This experimental design allowed us for assessing motor learning without the presence of augmented FB, that is, the control of movement relied mainly on proprioceptive information. Thus, the task was performed without any visual FB, or the performance was followed by visual FB after execution (i.e., a representation of the total trajectory).

2.3. Experimental design

Practice of the bimanual task was spread over 8 calendar days (see Fig. 1B). On day 1, the experiment consisted of 5 consecutive phases. (1) Participants looked at a white cross on the screen for 3 minutes to record the resting state with EEG, needed for estimating the task-related power (TRPower) (see Source analysis–Statistics). (2) We explained the task to the participants and they practiced unimanual movements to familiarize themselves with the setup; the unimanual movements consisted of rotations at similar speeds to the ones used in the bimanual conditions. (3) Following only instructions regarding the 3 different conditions (1:1, 2:5, and 5:2), participants executed the movements in the absence of augmented FB (i.e., no red line on the screen), hereafter referred to as baseline recording. EEG was recorded during execution. The 3 conditions were presented randomly in 3 blocks of 15 lines. Participants were instructed to perform the task as subtle as possible (using only the distal effectors) to avoid muscle artifacts in the EEG. (4) Practice started with provision of only after-trial FB (training 1). The conditions were presented repeatedly 5 times in blocks of 15 trials to aid learning within the first session. The order of conditions within each block was pseudorandomized across blocks. Whenever necessary, participants took breaks between blocks. The training session lasted about 30 minutes.

On trainings 2 and 3, corresponding to calendar days 3 and 5, participants continued to practice with after-trial FB. No FB trials were added (17% of the total number of trials) to let participants become familiar with executing the task in the absence of FB, and to reduce their dependence on augmented FB. The spacing of the calendar days was contingent on the scheduling of the sessions across weekdays.

On training 4, we started with the EEG recording for the resting-state condition and continued with the last practice session with after-trial FB. A 10-min break was given after practice was finished

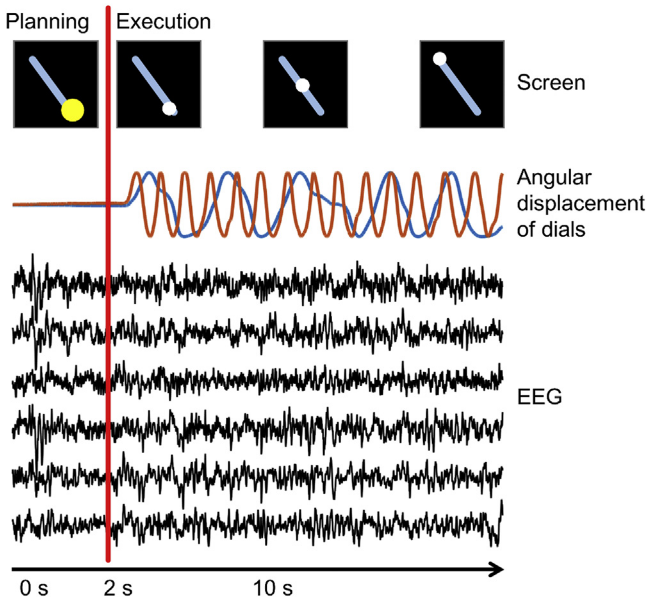

Fig. 2. Participants prepare the movement for 2 seconds after seeing the cue line on the screen. The start of the trial is indicated by the removal of the yellow circle in the center of the screen. A white dot moves along the cue line at a fixed speed. Participants execute the movement ratio without feedback. The angular displacement of a 2:5 ratio is shown across time. The EEG is recorded throughout the trial and the interval of task execution (after 2 seconds) is taken for further analysis. Abbreviation: EEG, electroencephalogram. (For interpretation of the references to color in this figure legend, the reader is referred to the Web version of this article.)

to continue with the retention test, which had the same characteristics as the baseline session, that is, random presentation of trials and no FB. The subsequent analyses focused on a comparison between the baseline and retention test sessions, whereby no after-trial FB was provided. The consistency of spectral measures using EEG has been shown after days and weeks (Cannon et al., 2012; Neuper et al., 2005).

2.4. Analysis of kinematics

To measure the level of performance, we calculated how well synchronized the movement of both hands was using the "coordination level," referred to as spectral overlap in previous studies (Daffertshofer et al., 2000; Houweling et al., 2010a; Press et al., 1994). Rotations of the dials were reconstructed by computing the sine of the angular displacement of each hand. The power spectral density of these sinusoids was determined using Welch's periodogram, with 4-s Hanning windows overlapping by 50%. The power spectral density was normalized by its maximum value. The coordination level measures how well and at what ratio both hand movements are frequency locked. It is defined as:

$$\Psi_x^y(\rho) = \frac{2\int P_x(f)P_y(\rho f)df}{\int\left[{P_x}^2(f)+{P_y}^2(\rho f)\right]df}$$

where P_x and P_y are the power spectral densities of the movement of each hand per trial, and ρ is a rescaling factor indicating the frequency ratio (e.g., for the frequency ratio 1:1, $\rho = 1$; and for 2:5, $\rho = 2.5$). The rescaling factor ρ was calculated from 0.1 to 6 with bins of 0.01. This was calculated per trial for all conditions.

To test whether participants had learned the task, we used a principal component analysis on the retention test per movement condition. Principal component analysis was applied on 3 matrices of 591 rows (bins of ρ) by 132 columns (3 blocks $\times$ 44 participants). Compared to the mere average, the first principal component has an associated "score," which represents the amount of variance from the whole data that the component explains. It can provide information regarding the ratio at which most participants were executing the task and the amount of variance from the data that it represents. The projection of the 1st principal component (with 132 elements) on the matrix of the coordination level was used to inspect at what frequency ratio most participants were truly synchronized (resulting in a vector of 591 elements per condition). By this, we could confirm that participants had acquired the target ratios during the retention test (see Behavioral results). The range of possible frequency ratios was based on a numerical approximation of low-order rational numbers (i.e., 2 decimals), which resulted in the range from 0.91 to 1.09 for the 1:1 ratio and from 2.41 to 2.59 for the nonisofrequency ratios. We averaged the coordination level within those ranges and obtained a single value per time point. The coordination level of trials in which the wrong hand was keeping the fast pace was set to the minimum, that is, zero. Because the 3 conditions were presented in blocks of 15 trials with 5 repetitions per condition, we divided each condition in blocks of 5 trials as they were presented. Hence, 3 blocks from the baseline session and 3 blocks from the retention test session, each comprising the average of 5 trials, were used for subsequent analysis. This analysis was conducted in MATLAB R2015b (The Mathworks, Natick MA, USA).

2.4.1. Statistics

In the traditional between-subject analysis of (co)variance and regression models, correlation of residuals in the models is not allowed. Given the between- and within-factors in our experimental design, we used a linear mixed-effects (LME) model (Pinheiro and Bates, 2000), which takes into account potential correlations of residuals within subjects. To assess the effect of learning and aging on the coordination level, we used an LME model that included 3 experimental variables (group, session, and frequency ratio) fitted as fixed factors and 1 random factor (subject). The group effect included the levels young and older adults; the session effect included the levels baseline and retention test; and the ratio effect included the levels 1:1, 2:5, and 5:2 using contrast coding. We used a full model including the three-way interaction and all constituent terms. For each level of ratio and session, we used the coordination level of 3 blocks, instead of averaging across blocks as frequently done in analyses of variance or t-tests. This preserved the intrasubject variability between blocks for a better fit of the model.

To evaluate the starting performance level of both groups and the level of learning at the end of the training, we used 2 additional models. One model was fitted with only the baseline blocks and included the variables group, ratio, and subject. To assess whether participants had reached a behavioral plateau in the last training days, we tested the effect of the last training days and the retention test and of aging on the coordination level, another model was fitted with the 3 last blocks of training 3 and training 4, and the blocks of retention test; this included the variables group, session, ratio, and subject.

The variance of the random factor for all models was estimated using restricted maximum likelihood. This analysis was conducted in R (version 3.3.1; www.r-project.org) and RStudio (version 0.99.903; www.rstudio.com) using the lme4 and lmerTest packages for LME modeling (Bates et al., 2015). We report the parameter estimates with Wald tests, sequential F-tests of fixed effects (type I sum of squares test), and variance component estimates for random effects. In LME, the null distribution of the test statistic is an approximation of the F-distribution, for which degrees of freedom need to be calculated directly from the data (Gałecki and Burzykowski, 2013). To correct for small sample bias, we used the Satterthwaite approximation (Bernal-Rusiel et al., 2013; Satterthwaite, 1946; Schaalje et al., 2002). Normality of the distribution of residuals was assessed by visual inspection.

2.5. EEG acquisition

EEG was recorded with a 128-channel amplifier (ANT, Enschede, Netherlands) with average reference. We used an elastic Waveguard cap with Ag/AgCl electrodes in the 10/5 standard layout. Eye movement was recorded with 2 bipolar electrooculography (EOG) channels. Electromyography (EMG) of left and right flexor carpi radialis was recorded with 2 bipolar channels. EEG, EOG, EMG signals and synchronizing triggers were amplified using the ANT Refa system and digitized at a rate of 1024 Hz. Locations of electrodes were digitized and recorded with an infrared Polaris Spectra camera (NDI, Ontario, Canada) in the neuronavigation Visor2 XT system (ANT).

2.6. MRI acquisition

A 3D high-resolution T1-weighted image of the participants' brain was obtained using a Philips Ingenia 3-Tesla CX MRI scanner with a standard head coil. A 3D-turbo field echo sequence was used (182 contiguous coronal slices, field of view = 250 $\times$ 250 mm^2, time echo = 4.6 ms, time repetition = 9.7 ms, time inversion = 1000 ms, slice thickness = 1.2 mm, in plane resolution = 0.98 $\times$ 0.98 mm^2).

2.7. Preprocessing of EEG data

EEG recordings of resting-state and task-related data were band-pass–filtered at 1–100 Hz and notch-filtered at 50 Hz. To minimize artifacts, 5 steps were taken. (1) Trials for artifact rejection in the task-related data were defined starting from the moment the cue line was shown on the screen (no movement) until the movement was finished (i.e., 10.5 seconds in total). Epochs for the resting-state EEG were redefined as 2-s segments. (2) Channels with voltage levels exceeding 150 μV were rejected. (3) Independent component analysis was applied to extract components related to eye blinks and movement artifacts. Components related to eye blinks/movements were selected based on the highest weights of the mixing matrix contributing to EOG channels. Components related to movement artifacts were selected based on their spectral properties, and their spatial and temporal kurtosis, similar to Nolan et al. (2010). Only components that contributed to more than 5% of the total data variance were rejected because noisy components were expected to contribute largely to the total variance (Delorme and Makeig, 2004). We reconstructed the data in sensor space by recombining the remaining components with their respective weights as estimated by independent component analysis. (4) Spectral characteristics of individual 200 ms windows with 50% overlap were obtained with the Welch's periodogram method (Welch, 1967). Spectral power in frequencies over 50 Hz and kurtosis were calculated in segments of 200 ms. The z-score was computed for these measures and segments with a z-score > 3 were identified as potential outliers and were considered for rejection. (5) The electromechanical delay (EMD) was determined for every trial as the lag corresponding to the maximum cross correlation of the low-pass–filtered rectified EMG signals and the angular displacement of the dials (Cavanagh and Komi, 1979). The EMD (lag) was used to synchronize the EEG and the angular displacement. Individual rotations of each hand were identified using the angular displacement and were mapped to the EEG time series, by shifting the EEG in time according to the EMD (Cavanagh and Komi, 1979). If the rotations lay on clean segments of the trial (no segments potentially noisy), they were selected as epochs for further processing, rendering at least 203 epochs in each participant (see Supplementary Table S5). These and further analyses were conducted using the Fieldtrip toolbox (Oostenveld et al., 2011) and customized MATLAB functions (R2015b).

2.8. Source analysis

Source estimation per frequency band of interest was performed using dynamic imaging of coherent sources (DICS) in combination with MRI-based individual head models. We used a mass-univariate LME model to assess the statistical effect of the individual experimental factors on power. Because we are not aware of any reports on EEG-derived markers of motor learning in aging, we considered a whole-brain analysis to provide the most comprehensive view on bimanual skill learning- and age-related changes in spectral power across the cortex.

2.8.1. Preparation of individual head models

In preparation for source estimation, individual head models were obtained from the MRIs. Individual head models yield a higher accuracy (Hallez et al., 2007; Liu et al., 2015). We used a 6-tissue finite element model for the skin, compact bone, spongy bone, cerebrospinal fluid, cortical and cerebellar gray matter, and cortical and cerebellar white matter using the Fieldtrip-SIMBIO integration toolbox (Buchner et al., 1997). To this end, we warped a high-resolution template of the human head and neck to the subject's space using the normalization tool in SPM12 (www.fil.ion.ucl.ac.uk/spm/software/spm12). This head template was obtained from the ITIS foundation of ETH Zurich (www.itis.ethz.ch/virtual-population/regional-human-models/mida-model/mida-v1-0) (Iacono et al., 2015). The conductivity values assigned for each compartment were 0.2, 0.0063, 0.04, 1.5385, 0.333, and 0.1429 Siemens/m, respectively, for the skin, the compact bone, the spongy bone, the cerebrospinal fluid, the gray and the white matter (Holdefer et al., 2006; Wagner et al., 2014; Wolters et al., 2006).

The position of the electrodes was aligned over the skin compartment by using the iterative closest point algorithm as implemented in SPM12. Next, a 3D grid with 5-mm spacing was created in the segmented volume corresponding to the cortical and cerebellar gray matter, which served as the locations of possible sources. The lead field was determined using the individual's finite element model head model, the electrodes' registered positions, and the 3D grid.

2.8.2. Source estimation

In general, DICS beamformers consist of adaptive spatial filters for each grid point that both pass signals from grid points with unit gain and maximally suppress signals from other sources (Gross et al., 2005). DICS beamformers are determined from the lead field matrix and the cross-spectral density matrix of all the electrode pairs. Importantly, by the use of the cross-spectral density matrix, the spatial filters are optimized to the statistical properties of the data, which increases the sensitivity of the reconstruction to small differences between conditions (Cohen, 2014). Adaptive spatial filters, such as DICS, exhibit higher spatial resolution when compared to nonadaptive filters (Greenblatt et al., 2005; Sekihara et al., 2005). In addition, DICS was applied as it has been successful for identifying source activity during bimanual movements (Houweling et al., 2010b; Pollok et al., 2005, 2014). The latter was calculated for the frequency bands of interest using the periodogram method with a Hanning window. All epochs were zero-padded to the maximum epoch duration to maintain the same resolution in the frequency domain. We used the alpha (8–12 Hz) and beta frequency bands (15–30 Hz), which are relevant bands for motor control and learning (Boonstra et al., 2007; Pfurtscheller and Lopes da Silva, 1999; Salmelin et al., 1995). These estimates were realized including the task-related and resting-state EEG data.

2.8.3. Statistics

Normalized power maps were spatially transformed to Montreal Neurologic Institute space and smoothed with a 6 × 6 × 6 mm Gaussian kernel by using SPM12. The TRPower was determined for every voxel with respect to the power during the resting state (Andres et al., 1999; Gerloff and Andres, 2002):

$$TRPower = \frac{Power_{movement} - Power_{rest}}{Power_{rest}}$$

A mass-univariate LME model was estimated across the whole brain using the Statistics and Machine Learning Toolbox of MATLAB, Version 10.1 (Mathworks, 2015) to extract sources that were modulated with learning and how these were different between both age groups. Following the marginality principle, the interpretation of the main effects is conditional in a model with interaction effects (Fox, 2015; Nelder, 1977). Therefore, we first fitted a full model including the interaction term of interest, and then fitted a (post hoc) model without the interaction term in voxels that did not surpass a statistical threshold of the interaction term.

2.8.3.1. Full model. The estimated model was defined as:

$$TRPower_{ij} = \beta_0 + \beta_1 Session_{ij} + \beta_2 Group_i + \beta_3 \boldsymbol{Group_i} \times \boldsymbol{Session_{ij}} + \beta_4 Baseline_i + \beta_5 Tempo_{relij} + b_{1i} + e_{ij}$$

which included fixed effects for the intercept (β_0), *Session* (β_1), *Group* (β_2), the *Group*Session* interaction (β_3); covariates to control for differences in performance during the baseline session (β_4) and for differences in movement speed (β_5) because our focus was on learning the coordination patterns (i.e., the coordination level), a random effect of the intercept (b_{1i}), which could vary per participant; and a residual error term (e_{ij}). The variable $Tempo_{rel}$ was calculated via:

$$Tempo_{rel}\ (\text{a.u.}) = \frac{d_{target} - d}{d_{target}}$$

where d_{target} was the length of the target line and d was the distance covered by the drawn line by the participant. If the drawn line was shorter than the target line, this indicated that the movement was slower than required. If the drawn line was longer than the target line, this indicated that the movement was faster than required.

Power maps per frequency ratio per day were included in the model. To facilitate the interpretation of the interaction term, however, in the EEG analysis, we focused on the neural correlates of learning, irrespective of frequency ratio, so it was not included in the model.

The variance of the random effect was estimated using restricted maximum likelihood. A linear hypothesis F-test was conducted on the *Group*Session* estimate (H_0: $\beta_3 = 0$). Similar to the statistical analysis of the behavioral data and for the models described next, we used the Satterthwaite approximation to calculate the degrees of freedom. We fitted the abovementioned model to the power maps in alpha and beta bands, calculated the corresponding F- and *p*-values, and pooled them to correct for multiple comparisons using the two-stage false discovery rate (FDR) approach (Benjamini et al., 2006) with an expected FDR threshold of 0.01. Only clusters larger than 1 cm^3 were kept for further analysis. This procedure was also followed for the main effects model described next.

In the interaction model, if the estimate for the variable *Group* is different from zero, there is a difference between groups during the Baseline session. We tested for this with the null hypothesis H_0: $\beta_2 = 0$. Regions of interest (ROIs) were selected from the thresholded F-maps based on the local maxima. We focused on these ROIs to present the results of the interaction model, but no additional models were fitted. Given that each estimate in the model has a corresponding confidence interval (based on the standard error of the mean [SEM]), we provided the predictions of the model fitted in the selected ROIs using the average covariates (*Baseline* and $Tempo_{rel}$) to visualize the direction of the interaction.

2.8.3.2. Post hoc model. Because we were also interested in the effects of *Session* and *Group* that did not interact, we selected the voxels that did not surpass the significance threshold in the first model with the *Group*Session* interaction and fitted a model with only the main effects by:

$$TRPower_{ij} = \beta_0 + \beta_1 \boldsymbol{Session_{ij}} + \beta_2 \boldsymbol{Group_i} + \beta_3 Baseline_i + \beta_4 Tempo_{relij} + b_{1i} + e_{ij}$$

We tested the linear hypothesis on *Session* (H_0: $\beta_1 = 0$) and *Group* (H_0: $\beta_2 = 0$). We corrected for multiple comparisons using an expected FDR threshold of 0.005. For all the models, the estimates of interest are reported as a percentage (i.e., *TRPower**100%).

For the interpretation of the spectral changes in the aforementioned models, decreases of power in the alpha and beta bands with respect to a baseline over sensorimotor areas are considered indexes of higher neural activity as they arguably occur with movement initiation and remain present during movement execution (Manganotti et al., 1998; Pfurtscheller, 2001; Pfurtscheller and Lopes da Silva, 1999; Pfurtscheller and Neuper, 1994; Stancák and Pfurtscheller, 1996). Therefore, the TRPower with respect to rest can be negative during higher activity.

In the results, we refrain from making strong statements about source estimation in the cerebellum and subcortical structures. Given the nature of the EEG signal, recording electrical activity from these areas is still a matter of debate (Dalal et al., 2014). From the selected ROIs, we fitted 2 additional models to investigate the relation of power changes with performance (see Supplementary File, Section S1).

3. Results

3.1. Behavioral results

During the retention test, participants executed the required ratios as shown by the projection of the 1st principal component on the coordination level data and the percentage of variance that is explained by the first component: 99%, 74%, and 74% for the 1:1, 2:5, and 5:2 ratios, respectively (Supplementary Fig. S1). The coordination level data for all the rescaling factors ρ revealed a reduced frequency locking at the nonisofrequency conditions for the older adults (see Fig. 3A). Hence, we averaged the coordination level within ranges of the rescaling factor ρ specified for each movement ratio (see dotted lines in Fig. 3A and Section 2.4).

The LME model including baseline and retention tests contained 792 observations (3 blocks × 3 ratios × 2 sessions × 44 participants) and revealed significant two-way interactions and significant main effects for *Group*, *Session*, and *Ratio* on the frequency overlap at the target ratios (see Fig. 3B, Tables 1 and 2). F-tests of sequentially fitted fixed effects revealed a significant effect of *Group* ($F_{(1,\ 41.97)} = 7.09$, $p = 0.012$) in which the older adults had a poorer performance (mean = 0.645; SEM = 0.0123) than the young adults did (mean [SEM] = 0.718 [0.01]). There was a significant effect of

Session ($F_{(1,736.05)}$=514.93, $p \leq 0.0001$) with an estimated improvement from the baseline session to the retention session of 0.2294 (0.0124). More specifically, the mean value was 0.5809 (0.0116) at the baseline and 0.789 (0.0079) during retention test. There was also a main effect of *ratio*, with the 1:1 ratio showing a better performance compared to the overall mean of all the ratios by 0.217 ($F_{(2,735.98)}$=226.06, $p \leq 0.0001$). The mean values for the different frequency ratios were 0.8223 (0.0034) for the 1:1 ratio, 0.6142 (0.0151) for the 2:5 ratio, and 0.6183 (0.0147) for the 5:2 ratio. There was a significant *Group*Session* interaction, whereby the older group improved their performance with training less than the young group by −0.0467 ($F_{(1,736.03)}$=6.61, $p = 0.01$), suggesting a learning deficit in older adults. The descriptive statistics for the *Group*Session* interaction were in young adults, 0.6036 (0.015) at baseline and increasing toward 0.8329 (0.0073) during the retention test and in older adults, 0.5533 (0.018) at baseline and 0.7359 (0.0139) during the retention test.

The LME model of the baseline blocks included 396 observations (3 blocks × 3 ratios × 44 participants) and showed a main effect of ratio on the coordination level at the target ratios; $F_{(2, 345.93)}$=384.59, $p < 0.0001$ (see Supplementary Table S1 and S2). The *Group*Ratio* interaction effect was not significant, but there was a trend for the 2:5 ratio; $t_{(345.9)} = -1.89$, $p = 0.059$, suggesting a slightly better performance in the young compared with the older adults during the execution of the 2:5 ratio at baseline. This trend was also present in the coordination level across different ratios (ρ) (see Fig. 3A) and in the coordination level averaged over the target ratio (see Fig. 3B).

The LME model of the training 3, training 4, and retention test included 1188 observations (3 blocks × 3 ratios × 3 sessions × 44 participants) and revealed an interaction effect of *Group*Ratio* ($F_{(2,1134)} = 53.03$, $p < 0.0001$) and a main effect of group on the coordination level at the target ratios ($F_{(1, 42)} = 16.15$, $p < 0.001$) (see Supplementary Table S3 and S4). That is, there was no effect of session in the last 2 training sessions and in the retention test because participants had reached a plateau in performance and likely started a consolidation stage.

In summary, the older group improved its performance less than the young group and exhibited poorer performance levels during the retention test than the young group (see Fig. 3B). There were larger performance improvements in the nonisofrequency conditions than in the isofrequency movement. Note, however, that we could not reject a similarity between groups at baseline. Both groups ultimately reached a plateau of performance at the end of the training sessions although the older group reached a lower performance level than the young group.

3.2. Electrophysiological results

3.2.1. Group*session interaction

Different electrophysiological changes underlying learning in the 2 age groups were found as shown by a significant *Group*Session* interaction (β_3 in the interaction model of source-estimated power) for different voxels and frequency bands. In the alpha band, voxels that showed the *Group*Session* effect extended to the right premotor ventral (PMV), the left lateral temporal lobe (LTL), occipital regions, and the cerebellum (see Fig. 4A; left). In the beta band, the regions showing this effect were the left ventromedial prefrontal cortex (VMPFC), right M1/S1 (dorsal), middle temporal lobe (MTL), and anteromedial prefrontal cortex (AMPFC), and bilateral posterior parietal cortex (see Fig. 4A; right).

As described in the Methods, ROIs were obtained based on the local maxima of the resulting F-maps (Fig. 4A) and were further inspected to evaluate the model estimates and the direction of the effect. The estimates of the coefficients and their respective statistics are summarized in Table 3.

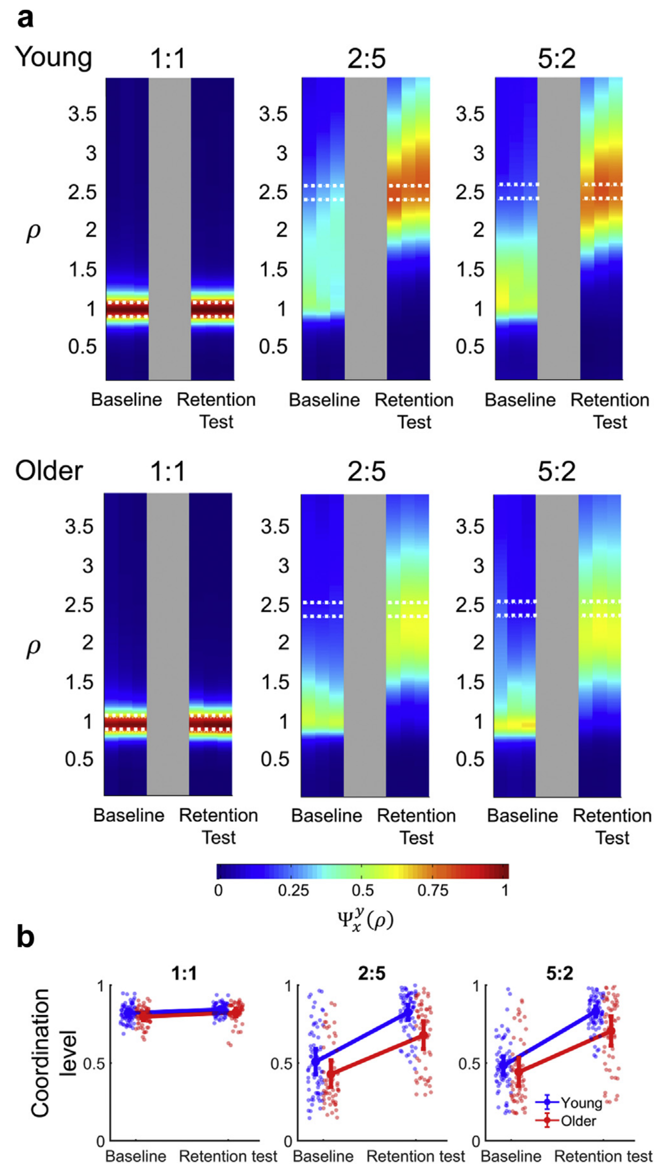

Fig. 3. (A) Averaged coordination level across different ratios (ρ) at conditions 1:1, 2:5, and 5:2 (reversed for visual representation) for the young (above) and the older group (below). Three blocks per session are shown. Each block is an average of 5 trials. Red color indicates strong coupling at the different ratios shown with decimals (ρ = [0.5, 1, 1.5, 2, 2.5, 3, 3.5] that relate to [2:1, 1:1, 2:3, 1:2, 2:5, 1:3, 2:7]). White dotted lines highlight the range selected for the target ratios. Please note the difference between groups in the spread of the coordination level during baseline for the ratio 2:5, indicating that the young group attempted to decouple the movement of the hands already in the baseline. (B) Coordination level at conditions 1:1, 2:5, and 5:2. The closer the value approximates 1 the better the performance. Blue: young group; red: older group. Error bars indicate the 95% confidence intervals for that particular session, group, and condition; the circle in the center of the error bars indicates the mean. Dots in the background indicate averages across blocks per participant. (For interpretation of the references to color in this figure legend, the reader is referred to the Web version of this article.)

Different patterns were found in the different ROIs and the different frequency bands. In the alpha band, in the right PMV, the young group showed a decrease of power with learning, whereas the older group showed an increase (see Fig. 5A). In the left LTL, both groups started with a similar power level at baseline but a more pronounced between-session increase of power was observed in the young group than in the older group.

In the beta band, the right M1/S1, AMPFC, MTL, the left VMPFC, and bilateral angular gyrus showed a lower power level for the

Table 1
LME estimates and Wald tests of behavioral data

Fixed effects	Estimate	SE	t (df)	p value
Intercept	0.6036	0.0194	31.19 (52)	<2E-16
Group older	−0.0503	0.0287	−1.75 (52.1)	0.0857
Session	0.2294	0.0124	18.54 (736)	<2E-16
Ratio 1:1 vs mean	0.2170	0.0124	17.54 (736)	<2E-16
Ratio 2:5 vs mean	−0.0964	0.0124	−7.795 (736)	2.2E-14
Group older*Session	−0.0467	0.0184	−2.54 (736)	0.0114
Group older*Ratio 1:1 vs mean	0.0268	0.0184	1.46 (736)	0.145
Group older*Ratio 2:5 vs mean	−0.0318	0.0184	−1.73 (736)	0.0846
Session*Ratio 1:1 vs mean	−0.2065	0.0175	−11.81 (736)	<2E-16
Session*Ratio 2:5 vs mean	0.0881	0.0175	5.03 (736)	6.08E-07
Group_older*Session*Ratio 1:1 vs mean	0.0509	0.0259	1.96 (736)	0.0502
Group_older*Session*Ratio 2:5 vs mean	−0.0175	0.0259	−0.67 (736)	0.5022

Random effects	Name	Variance	Std. Dev
Subject	Intercept	0.0072	0.0846
Residual		0.0165	0.1286

Above, estimates of fixed effects with their corresponding standard error of the mean (SE) and statistics of the individual estimates. Below, variance estimates of random effects.
Key: df, degrees of freedom; LME, linear mixed-effects.

older group at baseline and opposite patterns with learning: a decrease of power in the young and an increase of power in the older (see Fig. 5B).

3.2.2. Main effect of Session

Statistical tests for the *Session* term (β_1 in the main effects model of source-estimated power) revealed different brain areas. In the alpha band, the left LTL, medial prefrontal cortex (covering Brodmann Areas 11, 12, 32, 10), and precuneus showed an increase of power in the retention test compared to baseline (see Fig. 5B; left). The bilateral sensorimotor (ventral), premotor, and dorso-lateral prefrontal cortex showed a decrease of power after learning. The beta band showed the same effect for similar regions in addition to power decreases with practice in the right ventrolateral prefrontal cortex (see Fig. 5B; right).

3.2.3. Main effect of Group

Statistical tests of the *Group* term (β_2 in the main effects model of source-estimated power) revealed different brain areas for the alpha and beta bands. In both frequency bands, the *Group* effect consisted of lower power for the older group than the young group (see Fig. 5C). In the alpha band, this effect was restricted to the dorsomedial prefrontal cortex (DMPFC). In the beta band, this effect was widespread covering bilateral central lateral areas and medial prefrontal cortices in addition to the right insula.

4. Discussion

Using advanced EEG analysis methods, we investigated whole-brain changes in EEG spectral power associated with motor learning over 4 days of practice in young and older adults. Behaviorally, the older group showed less training-induced improvement and lower performance levels after practice than the young group. As expected, each group exhibited different changes in spectral power from the initial to the final stage of practice (*Group*Session* interaction). Specifically, we found a decrease of TRPower (increased neural activity) with practice in right (dorsal) M1/S1 in young adults, but no such changes in older adults. This possibly reflects a reduced plasticity of the central nervous system to implement lasting functional changes required for learning. In addition, common spectral effects of learning between the groups were present as TRPower decreases in the alpha and beta bands in bilateral (ventral) M1/S1, although not exclusively (main effect of *Session*). Alpha and beta power was lower in older compared with young adults in central and prefrontal cortices across time (main effect of group), potentially reflecting an overactivation. Overall, these results reveal heterogeneous age effects on the brain mechanisms associated with motor learning. To the best of our knowledge, this is the first study addressing the question of spectral changes in the context of aging, motor learning, and complex bimanual movements simultaneously.

Table 2
F-tests of sequentially fitted fixed effects of behavioral data (type I sum of squares test)

Effects of interest	Sum squares	Mean square	F (num df, den df)	p value
Group	0.117	0.117	7.09 (1, 41.97)	0.012
Session	8.510	8.510	514.93 (1, 736.05)	<2.2E-16
Ratio	7.471	3.735	226.02 (2, 735.98)	<2.2E-16
Group*Session	0.109	0.109	6.61 (1, 736.03)	0.0103
Group*Ratio	0.293	0.147	8.86 (2, 735.98)	1.575 E-4
Session*Ratio	3.344	1.672	101.15 (2, 735.98)	<2.2E-16
Group*Session*Frequency	0.066	0.033	1.99 (2, 735.98)	0.1379

Key: df, degrees of freedom; num, numerator; den, denominator.

4.1. Training-related changes in motor performance

The older group showed lower task performance than the younger group, consistent with previous findings showing an age-related deterioration of motor performance (Bangert et al., 2010; Bo et al., 2011; Seidler and Stelmach, 1995; Serbruyns et al., 2015; Shea et al., 2006; Solesio-Jofre et al., 2014; Summers et al., 2010; Swinnen et al., 1998). The isofrequency condition (1:1) was easier to perform than the nonisofrequency conditions for both groups, as shown previously for young adults with a similar task (Gooijers et al., 2013, 2016; Pauwels et al., 2014; Sisti et al., 2011). The *Group*Session* interaction indicated an overall lower performance improvement for the older group compared with the young group (Shea et al., 2006; Swinnen et al., 1998). Hence, the older group's learning potential was preserved, albeit to a lower extent than in young adults.

4.2. Differential training-related changes in spectral power as a function of age

The obtained heterogeneous spectral power results revealed that there is no single spectral pattern underlying motor learning in both age groups: there were both increases and decreases of power with practice in different brain regions and within different frequency bands in each group (*Group*Session* interaction). In general, differential neuronal mechanisms supporting motor learning in each age group were consistent with previous transcranial magnetic stimulation and fMRI reports (Aizenstein et al., 2006; Berghuis et al., 2016; Erickson et al., 2007; Lin et al., 2012). For most of the selected regions, the older adults started at a higher level of neural activity at baseline (lower spectral power) compared with young adults and then finished at a similar level in the retention test (due to training-induced decrease in spectral power in young adults). This neural difference may account for the learning deficit found in older adults. Mary et al. (2015) found no age-related effects in the beta band after practice of a motor sequence. The discrepancy with our findings may be due to the use of a bimanual task, which recruits wider neural areas and longer practice (4 days), which taps into longer term neuroplasticity.

Next, we focus on motor areas. For a discussion on other areas, see Supplementary Discussion. Starting at different power levels, the young adults exhibited decreased beta power in right M1/S1

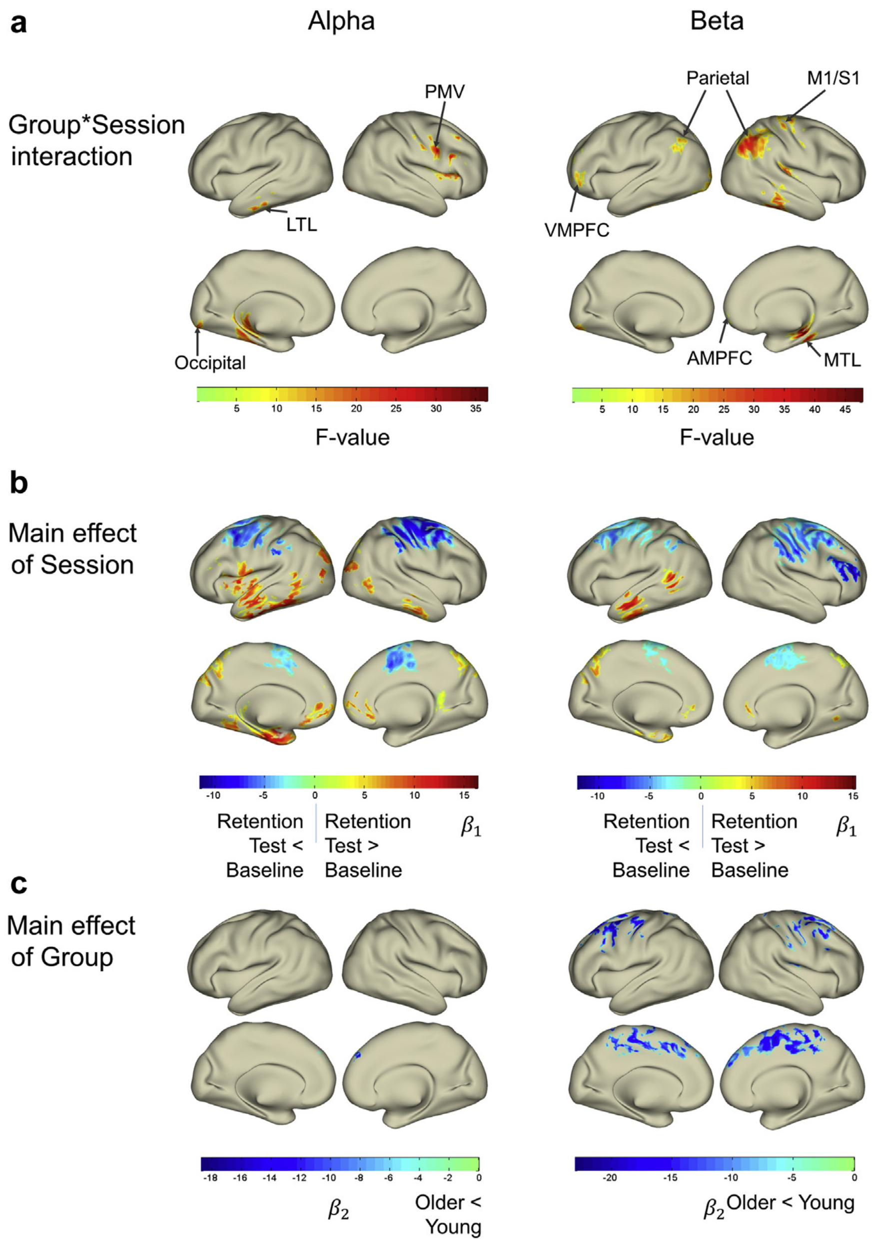

Fig. 4. Statistical results in the alpha (left) and beta (right) bands. (A) F-maps for the *Group*Session* (β_3) effect after controlling for an FDR of 0.01. (B) Beta-maps for the main effect of *Session* (β_1) and (C) the main effect of *Group* (β_2) after controlling for an FDR of 0.005. For the main effect of session, cold colors indicate significant voxels with lower task-related power in the retention test than in baseline; warm colors indicate significant voxels with higher task-related power in the retention test than in baseline. For the main effect of the group, color bar indicates significant voxels with lower task-related power in the older group than in the young group. Abbreviations: VMPFC, ventromedial prefrontal cortex; PMV, premotor ventral; LTL, lateral temporal lobe; AMPFC, anteromedial prefrontal cortex; M1/S1, sensorimotor cortices; MTL, medial temporal lobe. (For interpretation of the references to color in this figure legend, the reader is referred to the Web version of this article.)

(dorsal) with learning, whereas the older adults started at a lower level at baseline and remained at a similar level in the retention test. Heinrichs-Graham and Wilson (2016) suggested that TRPower decreases in the beta band, within subjects, are beneficial for performance up to a certain limit. The lower power found in older compared with young adults during baseline might be an age effect irrespective of performance or learning. With learning, TRPower decreases in M1/S1 could support performance improvements in young adults, whereas the lower power in the older adults during baseline would reduce the extent of potential learning-related effects in M1/S1 and its flexibility for adjusting to new skills. This could explain the older adults' learning deficit, as the decreased power (increased neural activity) that accompanies learning in young adults was absent in older adults. In line with this, we found a trend toward a negative relationship between the improvement in learning and changes in TRPower (see Supplementary Table S6). This relationship was borderline significant and did not survive correction for multiple comparisons, possibly due to the limited sample size. Additional confirmation is required in future studies.

There were practice-induced power decreases in the beta band in young adults, indicating an association of lower beta power with practice (and better performance). Conversely, lower power levels at baseline did not translate into better performance in older adults as seen in the right M1/S1 and PMV and also found in prefrontal and parietal areas (see Supplementary Discussion). Although highly speculative at this stage, this may suggest that aging affects the

Table 3
Coefficients of the interaction term Group*Session (β_3, the slope) for alpha and beta bands in selected ROIs

ROI label	MNI coordinates			Brodmann area	Fixed effect	Estimate	SE	F (num df, den df)	*p* value
	x	y	z						
Alpha									
PMV R	60	13	34	44	Group*Session	1.28	0.20	42.85 (1, 215.84)	4.25E-10
					Group	−1.23	0.52	5.51 (1, 45.1)	0.023382
LTL L	−54	−14	−35	20-22	Group*Session	−14.21	3.07	21.49 (1, 216.59)	6.14E-06
Occipital L	−12	−92	−17	18	Group*Session	24.79	5.22	22.54 (1, 216.43)	3.75E-06
Cerebelum Crus2 L	−12	−95	−38		Group*Session	23.49	4.13	32.39 (1, 216.65)	4.07E-08
Cerebellum 4 L	−21	−44	−23		Group*Session	−4.98	0.98	25.90 (1, 216.32)	7.8E-07
					Group	4.80	2.19	4.81 (1, 47.11)	0.033189
Beta									
M1-S1 R	40	−22	66	4, 3	Group*Session	5.13	1.19	18.51 (1, 216.07)	2.56E-05
					Group	−9.22	3.44	7.18 (1, 44.85)	0.010292
AMPFC R	6	73	−5	10, 11	Group*Session	13.37	2.79	22.94 (1, 216.52)	3.1E-06
					Group	−11.56	4.13	7.85 (1, 54.5)	0.007021
VMPFC L	−39	43	−8	47, 46	Group*Session	10.15	2.19	21.54 (1, 216.79)	6E-06
Parietal R	48	−71	46	39, 40	Group*Session	4.49	0.72	38.50 (1, 216.84)	2.74E-09
					Group	−2.54	1.06	5.73 (1, 55.14)	0.020104
Parietal L	−45	−56	34	39	Group*Session	9.83	1.99	24.39 (1, 216.51)	1.57E-06
					Group	−11.97	3.74	10.24 (1, 49.5)	0.002399
MTL R	39	−35	−8	37, 20	Group*Session	6.08	0.81	56.25 (1, 216.29)	1.63E-12
Cerebellum Crus1 L	−18	−95	−23		Group*Session	30.71	5.39	32.48 (1, 215.45)	3.93E-08

When relevant, the coefficients of the Group term (β_2, the intercept) are listed.
ROI labels as in Fig. 5.
Key: MNI, Montreal Neurologic Institute; PMV R, right premotor ventral; LTL L, left lateral temporal lobe; M1-S1, sensorimotor cortices; AMPFC R, right anteromedial prefrontal cortex; MTL R, right medial temporal lobe; VMPFC L, left ventromedial prefrontal cortex; SE, standard error of the estimate; df, degrees of freedom; num, numerator; den, denominator; ROI, region of interest.

underlying learning mechanism as expressed by neural overactivation when first faced with the task (baseline) and reduced/absent changes (trajectories) with practice (retention test–baseline). The minimal changes with practice found in older adults' right M1/S1 might be related to a lower capacity to recruit additional neural resources later in practice, given the high baseline recruitment.

4.3. Training-related EEG spectral power changes in both age groups

Similar training-induced power changes were observed across both age groups (main effect of session) in bilateral sensorimotor, premotor, prefrontal, and temporal areas in both alpha and beta bands. Here, we restrict the discussion to key areas of motor learning (see Supplementary Discussion for other areas). As hypothesized, practice yielded a decrease of task-related beta power in bilateral M1/S1, although in a more ventral location than the area found for the interaction effect. Previous studies on single-session practice reported beta power decreases in M/EEG scalp signals covering M1/S1 after bimanual and unimanual sequence learning (Andres et al., 1999; Cunha et al., 2006; Pollok et al., 2014) and bimanual polyrhythmic force production (Boonstra et al., 2007; Houweling et al., 2010b); however, no practice effects were found by Serrien and Brown (2003). We also found alpha power decreases in M1/S1 in agreement with previous reports in M/EEG scalp signals covering M1/S1 after bimanual sequence learning (Andres et al., 1999) and implicit learning of a unimanual sequence (Zhuang et al., 1997). Although these studies pertain to skill acquisition within a single session, our study extends this to multiday motor learning.

This practice-related decrease in beta power is consistent with invasive recordings obtained for longer term learning. Lower beta power in M1 has been associated with higher multiunit activity in pyramidal tract neurons in M1 that target the spinal cord (Baker et al., 2001; van Wijk et al., 2012). Studies of long-term learning (>30 days) in nonhuman primates report increases of firing rate or movement-related topography (Li et al., 2001; Matsuzaka et al., 2007; Recanzone et al., 1992). Our findings in M1 and premotor cortices are in agreement with fMRI studies reporting increased activity for these areas in the slow-phase of learning, that is, when automaticity has been achieved (Dayan and Cohen, 2011). M1 activity seems to increase after days or weeks of motor practice (Debaere et al., 2004; Floyer-Lea and Matthews, 2005; Hlustik et al., 2004; Karni et al., 1995; Puttemans et al., 2005), whereas left premotor activity increases after > 4-day practice regimes of a bimanual task (similar to the one used in this study) (Debaere et al., 2004; Puttemans et al., 2005).

4.4. Age-related differences in task-related EEG spectral power

Age-related effects on task-related EEG power were found mainly on centrolateral (M1/S1) and prefrontal regions for the beta band and in the DMPFC for the alpha band (main effect of group). Our findings of lower beta power in older adults in centrolateral regions agree with previous studies showing a decrease of mean movement-related beta power in M1/S1 across the full lifespan (Gaetz et al., 2010; Rossiter et al., 2014; Schmiedt-Fehr et al., 2016). However, we also found an extended spatial distribution of lower beta power in prefrontal areas and lower alpha power in DMPFC. The lower alpha and beta power in older adults reported here seems to indicate higher levels of information processing and/or higher involvement of the respective cortical areas during task performance.

The effect of age on brain activation during movement performance has been investigated in much detail using fMRI, revealing an involvement of additional brain areas and/or increased amplitude of the fMRI signal in the older as compared with young adults (e.g., Goble et al., 2010; Heuninckx et al., 2005, 2008, 2010; Santos Monteiro et al., 2017; Vallesi et al., 2011; Ward, 2006; Ward and Frackowiak, 2003). Older adults often recruit more prefrontal areas during complex movements, suggesting increased cognitive control during execution (Goble et al., 2010; Heuninckx et al., 2005,

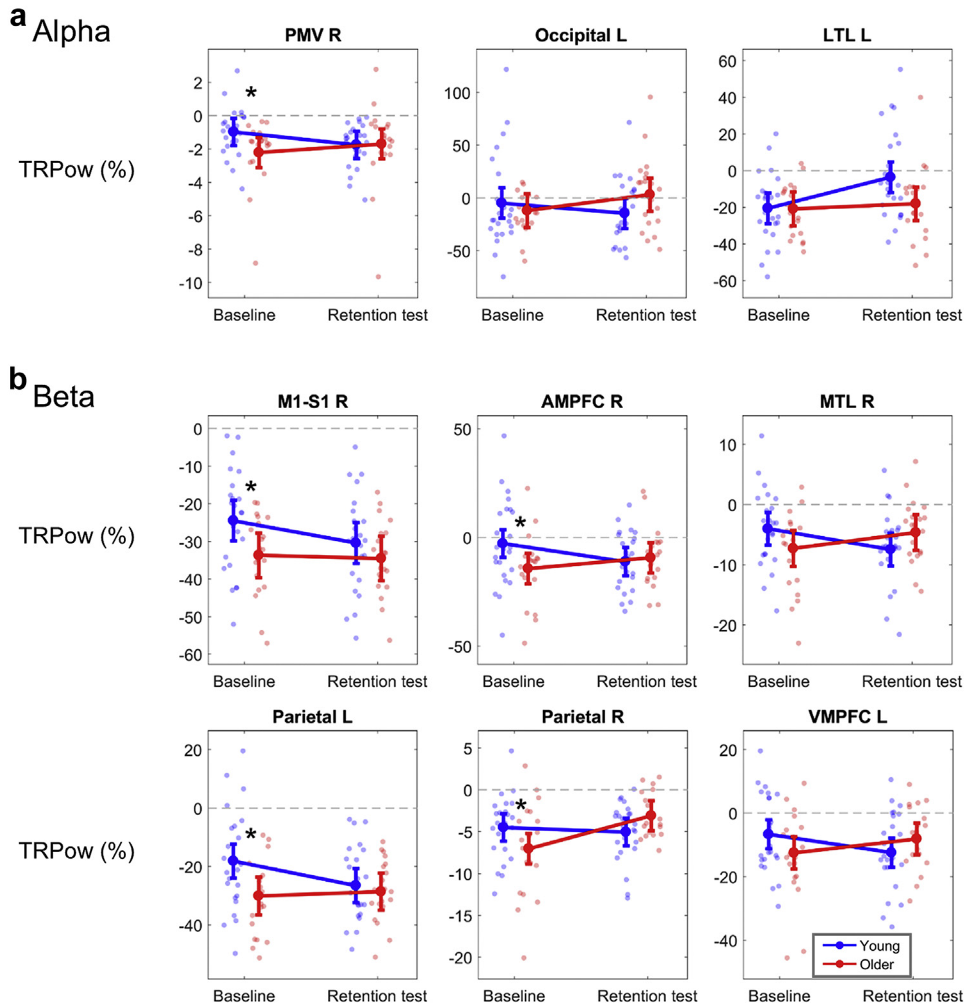

Fig. 5. Predictions of the interaction model with *Group**Session* (β_3, the slope) in ROIs from Fig. 4 in (A) alpha and (B) beta bands. Blue: young group; red: older group. Error bars indicate the confidence intervals of the prediction for the particular session and group. An asterisk indicates that the estimate for the fixed effect *Group* (β_2, the intercept) was significantly different from zero when controlling for an FDR of 0.05. Dots in the background indicate averages across conditions for each participant. Abbreviations: PMV R, right premotor ventral; LTL L, left lateral temporal lobe; M1-S1, sensorimotor cortices; AMPFC, anteromedial prefrontal cortex; MTL, medial temporal lobe; VMPFC L, left ventromedial prefrontal cortex; TRPow, task-related power; ROIs, regions of interest; FDR, false discovery rate. (For interpretation of the references to color in this figure legend, the reader is referred to the Web version of this article.)

2008). This may explain the lower alpha and beta power in prefrontal areas in older versus young adults in our results.

In conclusion, we provided a whole-brain investigation of changes in task-related EEG spectral power associated with age during training of a set of bimanual coordination tasks. Our results suggest that the compromised learning capacity found in older as compared with young adults may be related to a reduced neural plasticity, as indicated by smaller changes in sensorimotor and parietal task-related beta and alpha power. Moreover, the spectral power signature for age effects appears consistent with age-related overactivation found in fMRI studies. Taken together, adopting a broader perspective is warranted because age-related differences associated with learning can occur across the spectrum of frequency bands throughout the entire brain and in different directions across time.

Further research on the neural changes associated with normal aging is warranted. This may indeed serve as a benchmark for and improve our understanding of age-related neurodegenerative diseases (Johnson, 2015). We posit that the study of reduced learning capability and the associated brain activity alterations in healthy older adults may yield fundamental knowledge for an optimized treatment of motor deficits in older adults, including those with mild cognitive impairment, Parkinson's and Alzheimer's disease, among others.

Disclosure statement

The authors do not have actual or potential conflicts of interest.

Acknowledgements

The authors thank Prof. Genevieve Albouy, Dr. Quanying Liu, Paul Meugens, René Clerckx, Daniel Pérez Cardazo, and Johanna Moedden for their assistance. LMRD was supported by the European Commission through MOVE-AGE, an Erasmus Mundus Joint Doctorate programme (2011-0015). KFH was supported by the Internal Funding of the KU Leuven (OT/11/71 F+ fellowship, PDM/15/182). The work was partially supported by the KU Leuven Special Research Fund (grant C16/15/070) and the Research Foundation Flanders (FWO) (grants G0708.14, G0F76.16 and G0936.16) and Excellence of Science grant (EOS, 30446199, MEMODYN).

Appendix A. Supplementary data

Supplementary data to this article can be found online at https://doi.org/10.1016/j.neurobiolaging.2018.12.013.

References

Aburn, M.J., Holmes, C.A., Roberts, J.A., Boonstra, T.W., Breakspear, M., 2012. Critical fluctuations in cortical models near instability. Front. Physiol. 3, 331.

Aizenstein, H.J., Butters, M.A., Clark, K.A., Figurski, J.L., Andrew Stenger, V., Nebes, R.D., Reynolds III, C.F., Carter, C.S., 2006. Prefrontal and striatal activation in elderly subjects during concurrent implicit and explicit sequence learning. Neurobiol. Aging 27, 741–751.

Andres, F.G., Mima, T., Schulman, A.E., Dichgans, J., Hallett, M., Gerloff, C., 1999. Functional coupling of human cortical sensorimotor areas during bimanual skill acquisition. Brain 122, 855–870.

Baker, S.N., Spinks, R., Jackson, A., Lemon, R.N., 2001. Synchronization in monkey motor cortex during a precision grip task. I. Task-dependent modulation in single-unit synchrony. J. Neurophysiol. 85, 869–885.

Bangert, A.S., Reuter-Lorenz, P.A., Walsh, C.M., Schachter, A.B., Seidler, R.D., 2010. Bimanual coordination and aging: neurobehavioral implications. Neuropsychologia 48, 1165–1170.

Bates, D., Mächler, M., Bolker, B., Walker, S., 2015. Fitting linear mixed-effects models using lme4. J. Stat. Softw. 67, 48.

Beets, I.A.M., Gooijers, J., Boisgontier, M.P., Pauwels, L., Coxon, J.P., Wittenberg, G., Swinnen, S.P., 2015. Reduced neural differentiation between feedback conditions after bimanual coordination training with and without augmented visual feedback. Cereb. Cortex 25, 1958–1969.

Benjamini, Y., Krieger, A.M., Yekutieli, D., 2006. Adaptive linear step-up procedures that control the false discovery rate. Biometrika 93, 491–507.

Berghuis, K.M.M., De Rond, V., Zijdewind, I., Koch, G., Veldman, M.P., Hortobágyi, T., 2016. Neuronal mechanisms of motor learning are age dependent. Neurobiol. Aging 46, 149–159.

Bernal-Rusiel, J.L., Greve, D.N., Reuter, M., Fischl, B., Sabuncu, M.R., 2013. Statistical analysis of longitudinal neuroimage data with linear mixed effects models. NeuroImage 66, 249–260.

Bo, J., Peltier, S.J., Noll, D.C., Seidler, R.D., 2011. Age differences in symbolic representations of motor sequence learning. Neurosci. Lett. 504, 68–72.

Bönstrup, M., Hagemann, J., Gerloff, C., Sauseng, P., Hummel, F.C., 2015. Alpha oscillatory correlates of motor inhibition in the aged brain. Front. Aging Neurosci. 7, 193.

Boonstra, T.W., Daffertshofer, A., Breakspear, M., Beek, P.J., 2007. Multivariate time–frequency analysis of electromagnetic brain activity during bimanual motor learning. NeuroImage 36, 370–377.

Buchner, H., Knoll, G., Fuchs, M., Rienäcker, A., Beckmann, R., Wagner, M., Silny, J., Pesch, J., 1997. Inverse localization of electric dipole current sources in finite element models of the human head. Electroencephalogr. Clin. Neurophysiol. 102, 267–278.

Cahill, L., McGaugh, J.L., Weinberger, N.M., 2001. The neurobiology of learning and memory: some reminders to remember. Trends Neurosci. 24, 578–581.

Cannon, R.L., Baldwin, D.R., Shaw, T.L., Diloreto, D.J., Phillips, S.M., Scruggs, A.M., Riehl, T.C., 2012. Reliability of quantitative EEG (qEEG) measures and LORETA current source density at 30 days. Neurosci. Lett. 518, 27–31.

Cavanagh, P.R., Komi, P.V., 1979. Electromechanical delay in human skeletal muscle under concentric and eccentric contractions. Eur. J. Appl. Physiol. Occup. Physiol. 42, 159–163.

Cohen, M.X., 2014. Analyzing Neural Time Series Data: Theory and Practice. MIT Press, Cambridge, Massachusetts.

Cunha, M., Machado, D., Bastos, V.H., Ferreira, C., Cagy, M., Basile, L., Piedade, R., Ribeiro, P., 2006. Neuromodulatory effect of bromazepam on motor learning: an electroencephalographic approach. Neurosci. Lett. 407, 166–170.

Daffertshofer, A., Peper, C.E., Frank, T.D., Beek, P.J., 2000. Spatio-temporal patterns of encephalographic signals during polyrhythmic tapping. Hum. Mov. Sci. 19, 475–498.

Dalal, S.S., Rampp, S., Willomitzer, F., Ettl, S., 2014. Consequences of EEG electrode position error on ultimate beamformer source reconstruction performance. Front. Neurosci. 8, 42.

Davis, D.H.J., Creavin, S.T., Yip, J.L.Y., Noel-Storr, A.H., Brayne, C., Cullum, S., 2015. Montreal Cognitive Assessment for the diagnosis of Alzheimer's disease and other dementias. Cochrane Database Syst. Rev. 10, CD010775.

Dayan, E., Cohen, L.G., 2011. Neuroplasticity subserving motor skill learning. Neuron 72, 443–454.

Debaere, F., Wenderoth, N., Sunaert, S., Van Hecke, P., Swinnen, S.P., 2004. Changes in brain activation during the acquisition of a new bimanual coordination task. Neuropsychologia 42, 855–867.

Delorme, A., Makeig, S., 2004. EEGLAB: an open source toolbox for analysis of single-trial EEG dynamics including independent component analysis. J. Neurosci. Methods 134, 9–21.

Erickson, K.I., Colcombe, S.J., Wadhwa, R., Bherer, L., Peterson, M.S., Scalf, P.E., Kim, J.S., Alvarado, M., Kramer, A.F., 2007. Training-induced plasticity in older adults: effects of training on hemispheric asymmetry. Neurobiol. Aging 28, 272–283.

Floyer-Lea, A., Matthews, P.M., 2005. Distinguishable brain activation networks for short- and long-term motor skill learning. J. Neurophysiol. 94, 512–518.

Fox, J., 2015. Applied Regression Analysis and Generalized Linear Models, 3rd. ed. SAGE Publications Inc., Thousand Oaks, U.S.A.

Gaetz, W., MacDonald, M., Cheyne, D., Snead, O.C., 2010. Neuromagnetic imaging of movement-related cortical oscillations in children and adults: age predicts post-movement beta rebound. NeuroImage 51, 792–807.

Gałecki, A., Burzykowski, T., 2013. Linear Mixed-Effects Models Using R, A Step-by-step Approach, first ed. Springer-Verlag, New York.

Gerloff, C., Andres, F.G., 2002. Bimanual coordination and interhemispheric interaction. Acta Psychologica 110, 161–186.

Goble, D.J., Coxon, J.P., Van Impe, A., De Vos, J., Wenderoth, N., Swinnen, S.P., 2010. The neural control of bimanual movements in the elderly: brain regions exhibiting age-related increases in activity, frequency-induced neural modulation, and task-specific compensatory recruitment. Hum. Brain Mapp. 31, 1281–1295.

Gooijers, J., Beets, I.A.M., Albouy, G., Beeckmans, K., Michiels, K., Sunaert, S., Swinnen, S.P., 2016. Movement preparation and execution: differential functional activation patterns after traumatic brain injury. Brain 139, 2469–2485.

Gooijers, J., Caeyenberghs, K., Sisti, H.M., Geurts, M., Heitger, M.H., Leemans, A., Swinnen, S.P., 2013. Diffusion tensor imaging metrics of the corpus callosum in relation to bimanual coordination: effect of task complexity and sensory feedback. Hum. Brain Mapp. 34, 241–252.

Greenblatt, R.E., Ossadtchi, A., Pflieger, M.E., 2005. Local linear estimators for the bioelectromagnetic inverse problem. IEEE Trans. Signal Process. 53, 3403–3412.

Gross, J., Pollok, B., Dirks, M., Timmermann, L., Butz, M., Schnitzler, A., 2005. Task-dependent oscillations during unimanual and bimanual movements in the human primary motor cortex and SMA studied with magnetoencephalography. NeuroImage 26, 91–98.

Hall, S.D., Stanford, I.M., Yamawaki, N., McAllister, C.J., Rönnqvist, K.C., Woodhall, G.L., Furlong, P.L., 2011. The role of GABAergic modulation in motor function related neuronal network activity. NeuroImage 56, 1506–1510.

Hallez, H., Vanrumste, B., Grech, R., Muscat, J., De Clercq, W., Vergult, A., D'Asseler, Y., Camilleri, K.P., Fabri, S.G., Van Huffel, S., Lemahieu, I., 2007. Review on solving the forward problem in EEG source analysis. J. NeuroEngineering Rehabil. 4, 46.

Heinrichs-Graham, E., Wilson, T.W., 2016. Is an absolute level of cortical beta suppression required for proper movement? Magnetoencephalographic evidence from healthy aging. NeuroImage 134, 514–521.

Heuninckx, S., Wenderoth, N., Debaere, F., Peeters, R., Swinnen, S.P., 2005. Neural basis of aging: the penetration of cognition into action control. J. Neurosci. 25, 6787–6796.

Heuninckx, S., Wenderoth, N., Swinnen, S.P., 2008. Systems neuroplasticity in the aging brain: recruiting additional neural resources for successful motor performance in elderly persons. J. Neurosci. 28, 91–99.

Heuninckx, S., Wenderoth, N., Swinnen, S.P., 2010. Age-related reduction in the differential pathways involved in internal and external movement generation. Neurobiol. Aging 31, 301–314.

Hlustik, P., Solodkin, A., Noll, D.C., Small, S.L., 2004. Cortical plasticity during three-week motor skill learning. J. Clin. Neurophysiol. 21, 180–191.

Holdefer, R.N., Sadleir, R., Russell, M.J., 2006. Predicted current densities in the brain during transcranial electrical stimulation. Clin. Neurophysiol. 117, 1388–1397.

Houweling, S., Beek, P.J., Daffertshofer, A., 2010a. Spectral changes of interhemispheric crosstalk during movement instabilities. Cereb. Cortex 20, 2605–2613.

Houweling, S., van Dijk, B.W., Beek, P.J., Daffertshofer, A., 2010b. Cortico-spinal synchronization reflects changes in performance when learning a complex bimanual task. NeuroImage 49, 3269–3275.

Iacono, M.I., Neufeld, E., Akinnagbe, E., Bower, K., Wolf, J., Vogiatzis Oikonomidis, I., Sharma, D., Lloyd, B., Wilm, B.J., Wyss, M., Pruessmann, K.P., Jakab, A., Makris, N., Cohen, E.D., Kuster, N., Kainz, W., Angelone, L.M., 2015. MIDA: a multimodal imaging-based detailed anatomical model of the human head and neck. PLoS One 10, e0124126.

Jantzen, K.J., Fuchs, A., Mayville, J.M., Deecke, L., Kelso, J.A.S., 2001. Neuromagnetic activity in alpha and beta bands reflect learning-induced increases in coordinative stability. Clin. Neurophysiol. 112, 1685–1697.

Johnson, I.P., 2015. Age-related neurodegenerative disease research needs aging models. Front. Aging Neurosci 7, 168.

Karni, A., Meyer, G., Jezzard, P., Adams, M.M., Turner, R., Ungerleider, L.G., 1995. Functional MRI evidence for adult motor cortex plasticity during motor skill learning. Nature 377, 155–158.

Labyt, E., Cassim, F., Szurhaj, W., Bourriez, J.L., Derambure, P., 2006. Oscillatory cortical activity related to voluntary muscle relaxation: influence of normal aging. Clin. Neurophysiol. 117, 1922–1930.

Labyt, E., Szurhaj, W., Bourriez, J.L., Cassim, F., Defebvre, L., Destée, A., Derambure, P., 2004. Influence of aging on cortical activity associated with a visuo-motor task. Neurobiol. Aging 25, 817–827.

Li, C.-S.R., Padoa-Schioppa, C., Bizzi, E., 2001. Neuronal correlates of motor performance and motor learning in the primary motor cortex of monkeys adapting to an external force field. Neuron 30, 593–607.

Lin, C.-H., Chiang, M.-C., Wu, A.D., Iacoboni, M., Udompholkul, P., Yazdanshenas, O., Knowlton, B.J., 2012. Age related differences in the neural substrates of motor sequence learning after interleaved and repetitive practice. Neuroimage 62, 2007–2020.

Liu, Q., Balsters, J.H., Baechinger, M., van der Groen, O., Wenderoth, N., Mantini, D., 2015. Estimating a neutral reference for electroencephalographic recordings:

the importance of using a high-density montage and a realistic head model. J. Neural Eng. 12, 056012.
Lopes da Silva, F.H., 2006. Event-related neural activities: what about phase? In: Christa, N., Wolfgang, K. (Eds.), Progress in Brain Research. Elsevier, Amsterdam, pp. 3–17.
Lopes da Silva, F.H., 2010. EEG: origin and measurement. In: Mulert, C., Lemieux, L. (Eds.), EEG-fMRI: Physiological Basis, Technique, and Applications. Springer-Verlag, Berlin Heidelberg, p. 539.
Magill, R.A., 2007. Augmented Feedback, Motor Learning and Control: Concepts and Applications. McGraw-Hill, New York, USA, p. 482.
Manganotti, P., Gerloff, C., Toro, C., Katsuta, H., Sadato, N., Zhuang, P., Leocani, L., Hallett, M., 1998. Task-related coherence and task-related spectral power changes during sequential finger movements. Electroencephalogr. Clin. Neurophysiol. 109, 50–62.
Mary, A., Bourguignon, M., Wens, V., Op de Beeck, M., Leproult, R., De Tiège, X., Peigneux, P., 2015. Aging reduces experience-induced sensorimotor plasticity. A magnetoencephalographic study. NeuroImage 104, 59–68.
Mathworks, 2015. Matlab and Statistics and Machine Learning Toolbox Version 10.1 (R2015b). The MathWorks Inc., Natick, Massachussetts.
Matsuzaka, Y., Picard, N., Strick, P.L., 2007. Skill representation in the primary motor cortex after long-term practice. J. Neurophysiol. 97, 1819–1832.
Mattay, V.S., Fera, F., Tessitore, A., Hariri, A.R., Das, S., Callicott, J.H., Weinberger, D.R., 2002. Neurophysiological correlates of age-related changes in human motor function. Neurology 58, 630–635.
Mima, T., Matsuoka, T., Hallett, M., 2000. Functional coupling of human right and left cortical motor areas demonstrated with partial coherence analysis. Neurosci. Lett. 287, 93–96.
Moran, R.J., Kiebel, S.J., Stephan, K.E., Reilly, R.B., Daunizeau, J., Friston, K.J., 2007. A neural mass model of spectral responses in electrophysiology. NeuroImage 37, 706–720.
Muthukumaraswamy, S.D., Myers, J.F.M., Wilson, S.J., Nutt, D.J., Lingford-Hughes, A., Singh, K.D., Hamandi, K., 2013. The effects of elevated endogenous GABA levels on movement-related network oscillations. NeuroImage 66, 36–41.
Nasreddine, Z.S., Phillips, N.A., Bédirian, V., Charbonneau, S., Whitehead, V., Collin, I., Cummings, J.L., Chertkow, H., 2005. The Montreal cognitive assessment, MoCA: a brief screening tool for mild cognitive impairment. J. Am. Geriatr. Soc. 53, 695–699.
Nelder, J.A., 1977. A reformulation of linear models. J. R. Stat. Soc. Ser. A (General) 140, 48–77.
Neuper, C., Grabner, R.H., Fink, A., Neubauer, A.C., 2005. Long-term stability and consistency of EEG event-related (de-)synchronization across different cognitive tasks. Clin. Neurophysiol. 116, 1681–1694.
Nolan, H., Whelan, R., Reilly, R.B., 2010. FASTER: fully automated statistical thresholding for EEG artifact rejection. J. Neurosci. Methods 192, 152–162.
Oldfield, R.C., 1971. The assessment and analysis of handedness: the Edinburgh inventory. Neuropsychologia 9, 97–113.
Oostenveld, R., Fries, P., Maris, E., Schoffelen, J.-M., 2011. FieldTrip: open source software for advanced analysis of MEG, EEG, and invasive electrophysiological data. Intell. Neurosci. 2011, 1–9.
Pascual-Leone, A., Freitas, C., Oberman, L., Horvath, J.C., Halko, M., Eldaief, M., Bashir, S., Vernet, M., Shafi, M., Westover, B., Vahabzadeh-Hagh, A.M., Rotenberg, A., 2011. Characterizing brain cortical plasticity and network dynamics across the age-sSpan in health and disease with TMS-EEG and TMS-fMRI. Brain Topogr. 24, 302–315.
Pauwels, L., Swinnen, S.P., Beets, I.A.M., 2014. Contextual interference in complex bimanual skill learning leads to better skill persistence. PLoS One 9, e100906.
Pfurtscheller, G., 2001. Functional brain imaging based on ERD/ERS. Vis. Res. 41, 1257–1260.
Pfurtscheller, G., Lopes da Silva, F.H., 1999. Event-related EEG/MEG synchronization and desynchronization: basic principles. Clin. Neurophysiol. 110, 1842–1857.
Pfurtscheller, G., Neuper, C., 1994. Event-related synchronization of mu rhythm in the EEG over the cortical hand area in man. Neurosci. Lett. 174, 93–96.
Pinheiro, J.C., Bates, D.M., 2000. Mixed-effects Models in S and S-PLUS. Springer, New York.
Pollok, B., Latz, D., Krause, V., Butz, M., Schnitzler, A., 2014. Changes of motor-cortical oscillations associated with motor learning. Neuroscience 275, 47–53.
Pollok, B., Südmeyer, M., Gross, J., Schnitzler, A., 2005. The oscillatory network of simple repetitive bimanual movements. Cogn. Brain Res. 25, 300–311.
Press, W.H., Teukolsky, S.A., Vetterling, W.T., Flannery, B.P., 1994. Numerical Recipes in C: The Art of Scientific Computing, second ed. Cambridge University Press, Cambridge.
Puttemans, V., Wenderoth, N., Swinnen, S.P., 2005. Changes in brain activation during the acquisition of a multifrequency bimanual coordination task: from the cognitive stage to advanced levels of automaticity. J. Neurosci. 25, 4270–4278.
Ramón y Cajal, S., 1904. Textura del sistema nervioso del hombre y los vertebrados. Ed. Madrid, Imprenta de Nicolás Moya.
Recanzone, G.H., Merzenich, M.M., Jenkins, W.M., Grajski, K.A., Dinse, H.R., 1992. Topographic reorganization of the hand representation in cortical area 3b owl monkeys trained in a frequency-discrimination task. J. Neurophysiol. 67, 1031–1056.
Remy, F., Wenderoth, N., Lipkens, K., Swinnen, S.P., 2008. Acquisition of a new bimanual coordination pattern modulates the cerebral activations elicited by an intrinsic pattern: an fMRI study. Cortex 44, 482–493.
Ronsse, R., Puttemans, V., Coxon, J.P., Goble, D.J., Wagemans, J., Wenderoth, N., Swinnen, S.P., 2011. Motor learning with augmented feedback: modality-dependent behavioral and neural consequences. Cereb. Cortex 21, 1283–1294.
Rossiter, H.E., Borrelli, M.R., Borchert, R.J., Bradbury, D., Ward, N.S., 2015. Cortical mechanisms of mirror therapy after stroke. Neurorehabil. Neural Repair 29, 444–452.
Rossiter, H.E., Davis, E.M., Clark, E.V., Boudrias, M.H., Ward, N.S., 2014. Beta oscillations reflect changes in motor cortex inhibition in healthy ageing. NeuroImage 91, 360–365.
Rueda-Delgado, L.M., Solesio-Jofre, E., Mantini, D., Dupont, P., Daffertshofer, A., Swinnen, S.P., 2017. Coordinative task difficulty and behavioural errors are associated with increased long-range beta band synchronization. NeuroImage 146, 883–893.
Sailer, A., Dichgans, J., Gerloff, C., 2000. The influence of normal aging on the cortical processing of a simple motor task. Neurology 55, 979–985.
Salmelin, R., Forss, N., Knuutila, J., Hari, R., 1995. Bilateral activation of the human somatomotor cortex by distal hand movements. Electroencephalogr. Clin. Neurophysiol. 95, 444–452.
Salmelin, R., Hari, R., 1994. Characterization of spontaneous MEG rhythms in healthy adults. Electroencephalogr. Clin. Neurophysiol. 91, 237–248.
Santos Monteiro, T., Beets, I.A.M., Boisgontier, M.P., Gooijers, J., Pauwels, L., Chalavi, S., King, B., Albouy, G., Swinnen, S.P., 2017. Relative cortico-subcortical shift in brain activity but preserved training-induced neural modulation in older adults during bimanual motor learning. Neurobiol. Aging 58, 54–67.
Satterthwaite, F.E., 1946. An approximate distribution of estimates of variance components. Biometrics Bull. 2, 110–114.
Schaalje, G.B., McBride, J.B., Fellingham, G.W., 2002. Adequacy of approximations to distributions of test statistics in complex mixed linear models. J. Agric. Biol. Environ. Stat. 7, 512–524.
Schmidt, R.A., 1991. Frequent augmented feedback can degrade learning: evidence and interpretations. In: Requin, J., Stelmach, G.E. (Eds.), Tutorials in Motor Neuroscience. Springer Netherlands, Dordrecht, pp. 59–75.
Schmidt, R.A., Lee, T.D., 2011. The learning process, Motor control and learning- A behavioral emphasis, 5th edition. Human Kinetics, Champaign, IL, p. 592.
Schmiedt-Fehr, C., Mathes, B., Kedilaya, S., Krauss, J., Basar-Eroglu, C., 2016. Aging differentially affects alpha and beta sensorimotor rhythms in a go/nogo task. Clin. Neurophysiol. 127, 3234–3242.
Seidler, R.D., Stelmach, G.E., 1995. Reduction in sensorimotor control with age. Quest 47, 386–394.
Sekihara, K., Sahani, M., Nagarajan, S.S., 2005. Localization bias and spatial resolution of adaptive and non-adaptive spatial filters for MEG source reconstruction. NeuroImage 25, 1056–1067.
Serbruyns, L., Gooijers, J., Caeyenberghs, K., Meesen, R.L., Cuypers, K., Sisti, H.M., Leemans, A., Swinnen, S.P., 2015. Bimanual motor deficits in older adults predicted by diffusion tensor imaging metrics of corpus callosum subregions. Brain Struct. Funct. 220, 273–290.
Serrien, D., Brown, P., 2002. The functional role of interhemispheric synchronization in the control of bimanual timing tasks. Exp. Brain Res. 147, 268–272.
Serrien, D.J., Brown, P., 2003. The integration of cortical and behavioural dynamics during initial learning of a motor task. Eur. J. Neurosci. 17, 1098–1104.
Serrien, D.J., Cassidy, M.J., Brown, P., 2003. The importance of the dominant hemisphere in the organization of bimanual movements. Hum. Brain Mapp. 18, 296–305.
Shea, C.H., Park, J.-H., Wilde Braden, H., 2006. Age-related effects in sequential motor learning. Phys. Ther. 86, 478–488.
Sisti, H.M., Geurts, M., Clerckx, R., Gooijers, J., Coxon, J.P., Heitger, M.H., Caeyenberghs, K., Beets, I.A.M., Serbruyns, L., Swinnen, S.P., 2011. Testing multiple coordination constraints with a novel bimanual visuomotor task. PLoS One 6, e23619.
Solesio-Jofre, E., Serbruyns, L., Woolley, D.G., Mantini, D., Beets, I.A.M., Swinnen, S.P., 2014. Aging effects on the resting state motor network and interlimb coordination. Hum. Brain Mapp. 35, 3945–3961.
Stancák Jr., A., Pfurtscheller, G., 1996. Event-related desynchronisation of central beta-rhythms during brisk and slow self-paced finger movements of dominant and nondominant hand. Cogn. Brain Res. 4, 171–183.
Summers, J.J., Lewis, J., Fujiyama, H., 2010. Aging effects on event and emergent timing in bimanual coordination. Hum. Mov. Sci. 29, 820–830.
Swinnen, S.P., Lee, T.D., Verschueren, S., Serrien, D.J., Bogaerds, H., 1997. Interlimb coordination: learning and transfer under different feedback conditions. Hum. Mov. Sci. 16, 749–785.
Swinnen, S.P., Verschueren, S.M.P., Bogaerts, H., Dounskaia, N., Lee, T.D., Stelmach, G.G., Serrien, D.J., 1998. Age-related deficits in motor learning and differences in feedback processing during the production of a bimanual coordination pattern. Cogn. Neuropsychol. 15, 439–466.
Vallesi, A., McIntosh, A.R., Kovacevic, N., Chan, S.C.C., Stuss, D.T., 2010. Age effects on the asymmetry of the motor system: evidence from cortical oscillatory activity. Biol. Psychol. 85, 213–218.
Vallesi, A., McIntosh, A.R., Stuss, D.T., 2011. Overrecruitment in the aging brain as a function of task demands: evidence for a compensatory view. J. Cogn. Neurosci. 23, 801–815.
van Wijk, B.C.M., Beek, P.J., Daffertshofer, A., 2012. Neural synchrony within the motor system: what have we learned so far? Front. Hum. Neurosci. 6, 252.
Veldman, M.P., Maurits, N.M., Nijland, M.A.M., Wolters, N.E., Mizelle, J.C., Hortobágyi, T., 2018. Spectral and temporal electroencephalography measures

reveal distinct neural networks for the acquisition, consolidation, and interlimb transfer of motor skills in healthy young adults. Clin. Neurophysiol. 129, 419–430.
Voelcker-Rehage, C., 2008. Motor-skill learning in older adults—a review of studies on age-related differences. Eur. Rev. Aging Phys. Act. 5, 5–16.
Wagner, S., Rampersad, S.M., Aydin, Ü., Vorwerk, J., Oostendorp, T.F., Neuling, T., Herrmann, C.S., Stegeman, D.F., Wolters, C.H., 2014. Investigation of tDCS volume conduction effects in a highly realistic head model. J. Neural Eng. 11, 016002.
Ward, N.S., 2006. Compensatory mechanisms in the aging motor system. Ageing Res. Rev. 5, 239–254.
Ward, N.S., Frackowiak, R.S.J., 2003. Age-related changes in the neural correlates of motor performance. Brain 126, 873–888.
Welch, P., 1967. The use of fast Fourier transform for the estimation of power spectra: a method based on time averaging over short, modified periodograms. IEEE Trans. Audio Electroacoust. 15, 70–73.
Wolters, C.H., Anwander, A., Tricoche, X., Weinstein, D., Koch, M.A., MacLeod, R.S., 2006. Influence of tissue conductivity anisotropy on EEG/MEG field and return current computation in a realistic head model: a simulation and visualization study using high-resolution finite element modeling. NeuroImage 30, 813–826.
Zhuang, P., Toro, C., Grafman, J., Manganotti, P., Leocani, L., Hallett, M., 1997. Event-related desynchronization (ERD) in the alpha frequency during development of implicit and explicit learning. Electroencephalogr. Clin. Neurophysiol. 102, 374–381.